Transcriptomic Analysis Reveals Salt Tolerance Mechanisms Present in Date-Plum Persimmon Rootstock (*Diospyros Lotus*)

Francisco Gil_Muñoz
Instituto Valenciano de Investigaciones Agrarias
Nicolas Delhomme
Umea Universitet
Ana Quiñones
Instituto Valenciano de Investigaciones Agrarias
Maria del Mar Naval
Instituto Valenciano de Investigaciones Agrarias
Maria Badenes (badenes_mlu@gva.es)
Instituto Valenciano de Investigaciones Agrarias https://orcid.org/0000-0001-9722-6783
Rosario García Gil
Umea Universitet

Research article

Keywords: Diospyros lotus, salt stress, ion transport, photosynthesis, ROS signalling, root architecture

Posted Date: September 3rd, 2020

DOI: https://doi.org/10.21203/rs.3.rs-57244/v1

Abstract

Background Drought and salinity are two of the main challenges in agriculture. In many areas, crop production needs solutions to adapt the grown species to the increasing salinity. Research on physiological and molecular responses activated by salinity in plants is needed to elucidate mechanisms of salinity tolerance. Transcriptome profiling (RNA-Seq) is a powerful tool to study the transcriptomic profile of genotypes under stress conditions. In temperate fruit tree species, tree grafting on salinity tolerant rootstocks is a common method to compensate for the cultivar saline sensitivity. Persimmon species have different levels of tolerance to salinity, knowledge of this variability provides the basics for development of salt tolerant rootstocks.

Results In this study, we conducted a physiological and transcriptomic profiling of roots and leaves in tolerant and sensitive plants of persimmon rootstock, *Diospyros lotus*, grown under saline and control conditions. Results from characterization of the physiological responses along with gene expression changes in roots and leaves allowed identifying several salt-tolerance mechanisms related to Ion transport and thermospermine synthesis. Differences were observed in putative H^+/ATPases that allow transmembrane ionic transport and Chloride channel protein-like genes. Furthermore, an overexpression of thermospermine synthase found in the roots of tolerant plants may indicate that alterations in root architecture could act as an additional mechanism of response to salt stress.

Conclusions Results indicate that *D. lotus* presents a genetic variability for salt tolerance trait related to the regulation of chloride transport, transmembrane electrochemical potential and thermospermine root synthesis. The study provides knowledge on mechanism of salt stress tolerance in persimmon for further breeding of tolerant persimmon rootstocks.

Background

Drought and salinity are two of the main challenges in agriculture. Reduction of water availability and increase of salinity in soils and water reservoirs can limit crop production due to severe inhibition of plant growth and development via osmotic and ionic stresses (1, 2). The negative effect of salinity in photosynthesis is caused either by a reduction in available water, by the toxic accumulation of ions in the cell, or both. Furthermore an attenuated photosynthesis leads to an increase in Reactive Oxygen Species (ROS) and a consequent oxidative damage of the cells (3). The cultivated surface affected by either stresses increases year after year as a consequence of more frequent drought episodes associated to climate change. Among the affected areas, the Mediterranean basin registered a significant increase in salinity in soils and water reservoirs in the last 10 years (4). Therefore, there is a pressing need to find solutions to alleviate the negative impact on plant production in an area dominated by fruit tree crops. Controlled crosses and selection (plant breeding) has proven an efficient method to develop new cultivars with improved characteristics such as salinity tolerance in several species (5–8). In the case of temperate fruit trees, salinity stress can also be overcome by means of tree grafting on tolerant rootstocks (9). This method provides a solution for dealing with the two components of salinity stress: the osmotic effect, or

water balance loss, through decreasing the area of stomatal aperture via phytohormonal root signalling (10, 11) and ionic toxicity, by maintaining the ion homeostasis in the cell of the aerial parts (12). Furthermore, grafting of existing varieties on rootstocks contributes to avoid losing the current genetic diversity.

Previous studies have contributed knowledge about the molecular mechanisms that regulate plant´s physiological responses to salinity in both model and economically important crops (13–15). Those mechanisms involve changes in gene expression associated to several biological processes such as ionic transport and exchange mechanisms (16), photosynthesis (17), flavonoid biosynthesis (18), ROS scavenging and detoxification (19), ethylene production (20), signalling networks related to ABA (Abscisic Acid) (21) and protein refolding (22). Expression of different functional genes related to osmoregulation and cell protection as dehydrins and aquaporins are involved as well in salinity response (22–24).

One of the most prompt physiological response following exposure to saline environments is the differential regulation of growth water balance and uptake, and the activation of different cascades of molecular networks that result in the expression changes of specific stress-related genes, and their encoded metabolites (25, 26). Studies focused on model plants revealed the involvement of several transduction pathways in salt stress response, including SOS (Saline Overly Sensitive) (27), ABA (11) and ethylene signaling pathways (28). Additional cell wall changes result in differential growth responses required to adapt to saline environments (29). Significant amount of data concerns the role of plant mitogen-activated protein kinases (MAPKs) in osmoregulation. MAPK cascades are now recognized as major signal transduction mechanisms to regulate gene expression, multiple cell activities and protein functions in various developmental and adaptive processes (30), including salt stress (31). Ion toxicity caused by Na^+ and Cl^- accumulation also affects plant photosynthesis, which can lead to leaf and stem necrosis. Mechanisms to limit Na^+ uptake and translocation are therefore linked to salinity tolerance. Several genes have been identified in *Arabidopsis*, such as the Na^+/H^+ antiporter responsible for the exclusion of sodium from the cytosol (32) in the SOS response pathway. In *Arabidopsis thaliana*, the serine/threonine type protein kinase SOS2 (CBL-interacting serine/threonine-protein kinase 24) interacts with the calcium sensor SOS3 (Calcineurin B-like protein 4) to regulate the Na^+/H^+ antiporter SOS1, thereby conferring salt tolerance (33, 34). Na^+/K^+ homeostasis in poplar is regulated by CIPK (CBL-interacting serine/threonine-protein kinase) genes which interact with CBL1 (Calcineurin B-like protein 1) (35). The CIPK genes from wild barley and maize are also known to be implicated in salt tolerance responses (36, 37). Furthermore, in tolerant persimmon species such as *Diospyros virginiana*, salt stress tolerance is believed to be caused by a high affinity potassium transporter *HKT-1-like* gene in roots (38), which was previously described in other species as key factor in salinity tolerance (39–42). Although Na^+ ion translocation and regulation mechanisms have previously been reported in several species, little is known about Cl^- transport and regulation. It has been suggested that Cl^- uptake occurs mainly through passive water intake (2), although chloride channels are also suggested to be able to sequestrate Cl^- ions (43). Chloride accumulation effect is also especially important in persimmon where it causes a decrease in fruit quality and a shorter post-harvest life (44).

In this study, the main objective is aimed at unravelling the mechanism of salinity tolerance in persimmon rootstock. Persimmon species have different levels of tolerance to salinity, making them an appropriate model to study the mechanisms of salinity tolerance, and to provide knowledge on persimmon species´ potential as salt tolerant rootstock. Transcriptome profiling (RNA-Seq) using next-generation sequencing technologies has proven a powerful tool to detect changes in gene expression associated to physiological responses to salt stress (45–49). In this study, we conducted physiological and RNA-Seq analyses of roots and leaves in persimmon rootstocks (*Diospyros lotus*) grown under saline and control conditions.

Results

Plant physiological responses associated to salt stress tolerance

Plants exposed to saline treatment showed significant reduction in growth, increased leaf damage and defoliation, and altered ion concentration. Among the treated plants, those physiological responses were especially pronounced in a subset of plants which we hereafter categorized as sensitive to salinity (Table 1). As compared to tolerant plants the sensitive ones showed a significantly higher Cl^- concentration. Interestingly, no significant differences were observed for Na^+ accumulation, neither were differences significant for Na^+/K^+ and Na^+/Ca^{2+} ratios. Moreover, P accumulation was more pronounced in tolerant plants. The overall reduction in carbon fixation capacity and water potential due to salinity were significantly more pronounced in the sensitive plants.

The morphological differences between tolerant and sensitive plants were significant for the Relative Growth Rate (RGR) (Figure 1). The sensitive plants showed less RGR than the tolerant ones at the end of the saline treatment (day 60).

Gene expression changes in response to salinity

To visualise the gene expression profiling results, a principal component analysis (PCA) was conducted using the transcriptomic data for all samples. In this analysis, a clear separation was observed between roots and leaves. Leaves showed little variability between the three categories (Figure 2). However, the percentage of variability explained between control and treated roots was of the same order of magnitude as that between leaves and roots. Furthermore, the separation between tolerant and sensitive plants was also significant based on root transcriptomic data as shown in Figure 2. This separation was consistent with the phenotypic data presented above.

The comparison between expression in tolerant *vs* sensitive plants revealed 2901 differentially expressed genes. These genes were further filtered using the BLAST results and annotations to look for putative genes related to salinity tolerance. Additionally, an orthogonal design analysis was conducted to be able to differentiate gene expression differences specific to roots or to leaves. The orthogonal analysis identified 1277 genes differentially expressed between tolerant and sensitive leaves (Supplementary

figure 1). Also, 1395 genes were differentially expressed between tolerant *vs* sensitive roots (Supplementary figure 2).

Differentially expressed genes were divided according to several salt-tolerance mechanisms: ion transport, photosynthesis and respiration systems, and ROS detoxification. No water transport related genes were found differentially expressed. Ion transport related genes were divided according to each ion type (Table 2). Among Ca^{2+} transport related genes, a calcium ATPase-like gene was down-regulated in the leaves of sensitive plants as compared to those in tolerant plants, whereas the opposite was true for the roots. Furthermore, a calcium uniporter protein-like gene was found to be upregulated in the leaves of sensitive plants. Potassium channels SKOR and KAT3-like genes were downregulated in the leaves of sensitive plants, whereas a probable potassium transporter was upregulated in the leaves of sensitive plants. With regard to ionic channels, vacuolar cation/proton exchangers were upregulated in the leaves of sensitive plants. Other cation/proton antiporters did not show a clear response to salinity stress, as some isoforms had different expression patterns. On the other hand, chloride channel protein-like genes were upregulated in both leaves and roots of sensitive plants and downregulated in tolerant leaves. Phosphate, magnesium and boron transport-related genes were upregulated in tolerant roots. Phosphate, zinc and ammonium transport-related genes were also upregulated in tolerant leaves. Regarding ATPases, Plasma membrane ATPase-like genes were strongly upregulated in the roots of tolerant plants and downregulated in sensitive leaves. Furthermore, a V-type proton ATPase subunit G-like gene was strongly upregulated in leaves of tolerant plants as compared to the sensitive ones.

Include here Table 2

Regarding photosynthesis and respiration genes, all genes were downregulated in roots from all plants in comparison to the leaf expression levels (Table 3). Differentially expressed genes in leaves were all upregulated in the tolerant plants as compared to the sensitive ones, while the expression levels of the tolerant plants were similar to the control plants.

Log2 FC and adjusted p-value for genes associated to photosynthesis and respiration which are differentially expressed in tolerant vs sensitive plants. Colors represent relative differences in expression according to the read counts: red color is assigned to the lowest count value and blue color is assigned to the highest count value. Leaves and roots are represented by the columns with letters “L” and “R”. Brown columns correspond to the relative mean expression in control plants, blue tolerant plants and red sensitive plants. Tissue column indicates tissue specificity of the tolerant vs sensitive expression

Concerning the ROS detoxification related genes (Table 4), all except Thermospermine synthase ACAULIS5-like presented a higher expression in the leaves. Peroxiredoxin-like and peroxidase-like genes were upregulated in the tolerant plants except for one peroxidase-like that was upregulated in sensitive plants. Thermospermine synthase ACAULIS5-like was strongly upregulated in the roots of the tolerant plants and strongly downregulated in the leaves of the sensitive plants.

Log2 FC and adjusted p-value for genes associated to photosynthesis and respiration which are differentially expressed in tolerant vs sensitive plants. Colors represent relative differences in expression according to the read counts: red color is assigned to the lowest count value and blue color is assigned to the highest count value. Leaves and roots are represented by the columns with letters “L” and “R”. Brown columns correspond to the relative mean expression in control plants, blue tolerant plants and red sensitive plants. Tissue column indicates tissue specificity of the tolerant vs sensitive expression.

Table 1
Physiological responses under control and saline conditions.

	Non-saline			Saline					
	Control			Sensitive			Tolerant		
Initial height (cm)	11.5	±	1.4	14.9	±	1.1	12.8	±	1.4
Initial node number (nº)	4.7	±	0.6	5.0	±	0.0	5.0	±	0.0
Initial internode length (cm)	2.5	±	0.4	3.0	±	0.2	2.6	±	0.3
Final height (cm) *	76	±	20	28	±	4	39	±	2
Final node number (nº) *	35	±	6	19.0	±	1.0	24	±	3
Final internode length (cm)	2.2	±	0.4	1.47	±	0.18	1.62	±	0.14
Defoliation (leaves/nodes) *	0.0	±	0.0	0.33	±	0.13	0.12	±	0.03
Stem water potential (MPa) *	-0.82	±	0.16	-0.35	±	0.05	-0.73	±	0.06
ACO_2 (µmol CO_2/m^2s) *	11.3	±	3.1	1.1	±	1.3	9.2	±	0.9
g_s (mmol H_2O/m^2s) *	254	±	262	40	±	21	242	±	74
C_i (µmol CO_2/m^2s)	254	±	59	357	±	47	306	±	15
WUE (µmol CO_2/mol H_2O) *	70	±	4	20	±	20	40	±	10
Cl^- (mg/g d.w.) *	0.49	±	0.09	5.5	±	0.2	4.0	±	0.3
Ca^{2+} (mg/g d.w.)	0.63	±	0.07	0.32	±	0.06	0.42	±	0.08
K^+ (mg/g d.w.)	1.6	±	0.2	0.99	±	0.19	1.4	±	0.3
Mg^{2+} (mg/g d.w.)	0.179	±	0.013	0.17	±	0.02	0.21	±	0.04
Na^+ (mg/g d.w.)	0.21	±	0.07	4.9	±	0.3	5.0	±	1.4
P (mg/g d.w.) *	0.064	±	0.016	0.12	±	0.01	0.15	±	0.02
S (mg/g d.w.)	0.12	±	0.02	0.06	±	0.02	0.07	±	0.02
Na^+/K^+	0.13	±	0.04	5.1	±	1.2	3.63	±	0.18
Na^+/Ca^{2+}	0.34	±	0.14	15.9	±	4.3	11.8	±	1.2

Asterisk (*) indicates significant differences between tolerant and sensitive groups (Kruskal-Wallis test, $p < 0.05$).

Discussion

Ion Transport

Following salt treatment, no significant differences between salt tolerant and sensitive plants were observed for Na^+, Ca^{2+} or K^+ accumulation in leaves. However, a higher K^+ and Ca^{2+} accumulation in the leaves of tolerant plants coincides with a higher leaf expression of several potassium channels and calcium transporting ATPases in the tolerant plants.

In our study, the total content of Na^+ and Cl^- was analysed and therefore a possible vacuolar compartmentalization could not be detected. However, we observed higher expression of all the analysed H^+-ATPases in tolerant plants. This suggest the involvement of these genes in the compartmentalization mechanism of cell protection from Na^+ toxicity. In spite of that the responsible proteins of the removal of sodium ions from the cytoplasm into the apoplast or vacuole are the specific plasma membrane Na^+/H^+ antiporters, the activity of this protein depends on the electrochemical proton gradient between membranes. The H^+-ATPases are the only proteins that are able to generate the adequate electrochemical proton gradient that allows these antiporters to perform the Na^+ extrusion (50). Furthermore, the upregulation of this protein under salt conditions has been previously reported (51–54) and its critical role on the Na^+ extrusion has been confirmed using transgenic plants (55,56).

Another ion directly involved in damage caused by toxicity is Cl^-, especially in the case of persimmon as previously shown by others (44,57). Previously, we detected differential chloride accumulation in the D. lotus population from the plants were obtained (58), however we could not link any previously measured parameter to these phenotype. In our study, we have observed a direct relationship between expression of chloride channel proteins and chlorine accumulation in leaf. Recently, chloride channels were proposed as key transporters of Cl^- into the higher parts of the plant (43). In persimmon, our results suggest that these channels might be playing a key role in avoiding high Cl^- leaf accumulation in tolerant plants.

Photosynthesis, respiration systems and ROS signalling

A decreased metabolism in sensitive plants is supported both by the downregulation of photosynthetic and respiratory genes, and by a significant reduction in carbon fixation. This effect might be caused by a combination of reduced transpiration and cell damage caused by the accumulation of toxic ions causing leaf necrosis and defoliation (2). ROS inactivation is also higher in both control and tolerant leaves an effect that probably leads to higher leaf ROS content in the sensitive plants. Although ROS can cause toxic effect in the leaves, it is a part of a signalling mechanism that may not be key to explaining the salinity tolerance, as an efficient ROS detoxification is essential for plant survival under natural conditions (2). ROS are known to trigger programmed cell death (59) and tissue necrosis and defoliation, which are believed to be a mechanism for protecting the most photosynthetically active cells (60).

Root architecture involvement

Under stress conditions, thermospermine synthesis and K^+ uptake are linked to the inhibition of lateral root formation (61,62). Although root architecture was not characterized in this study, transcriptomic data revealed thermospermine synthesis and K^+ transport activation by salinity in roots of tolerant plants, which suggests that root architecture may also play a role in the mechanism of tolerance to salt stress. Although previous reports have pointed out the association between reduced lateral root growth and sensitivity to saline stress trough better maintenance of Na^+/K^+ ratio by accumulating Na^+ in the secondary root stele (63), other studies have pointed that in some cases, such as in seedlings, accumulation of Na^+ in the stele can cause lateral root quiescence or even lateral root primordia damage (64) and therefore reduced root development. In this line, *D. virginiana*, which is considered a salt-tolerant persimmon rootstock the root system is characterized by a well-developed taproot (65). *D. lotus*, a salt-sensitive rootstock, is characterized by a fibrous root system as compared to *D. virginiana* that presents a well-developed taproot (66), this morphological differences are believed to play an important role in the salinity tolerance in *Diospyros* rootstocks (67). Our expression results indicate a possible association between root architecture and tolerance to salinity warrants further studies.

Conclusions

To sum up, in *Diospyros lotus* several mechanisms are present to overcome the saline stress. In this paper we could elucidate the ones that present variability within these species and therefore could be exploited for breeding new salt-tolerant rootstocks. At root level, thermospermine might play a role in root architecture, whose involvement in salt tolerance among *Diospyros* species has been previously pointed by other authors (67). On the other hand, chloride channel expression could facilitate Cl^- transport inside the plant, and therefore cause higher Cl^- accumulation in the higher parts of the plant. Finally, in the leaves, H^+-ATPases seems to be crucial to be able to generate the electrochemical membrane gradient to allow Na^+ extrusion from the cytoplasm.

Methods

Plant material and RNA extraction

In this study we used a full-sib progeny of *Diospyros lotus* (DL) obtained from a cross between two *D. lotus* trees that belong to the Instituto Valenciano de Investigaciones Agrarias (IVIA) persimmon germplasm collection (accession number DK034). Identification of the plant material was made by the IVIA. Botany information and accessions are publicly available at *https*://www.gva.ivia.es. Seeds were stratified in plastic bags filled with perlite in a cold chamber at 4ºC at the end of March. After 30 days of stratification, seeds were transferred to peat-moss and perlite (4:1 ratio) and transferred to a greenhouse at 18-24ºC during two months (from April, 24, to June, 26, 2017).

One hundred and fifty seedlings were transplanted into 1L pots filled with coarse sand. Plants were acclimatized in the greenhouse until apical meristem growth was observed. During this period, the plants

were watered with a nutrient solution (3% Cristaljisa 18-18-18, soluble fertilizer with micronutrients). The plants were distributed randomly in the greenhouse to avoid possible biases. The plants were acclimated before exposition to salinity treatment. After acclimation, plants were exposed to saline stress treatment during 60 days. The saline stress consisted in adding 40 mM NaCl to the nutrient solution. Control plants remained watered with only nutrient solution.

Three of the plants were kept in control treatment, and six treated plants (three tolerant, three sensitive) seedlings were selected based on salt tolerance according to the visual and agro-morphological data, aspect of tolerant and sensitive plants are in supplementary figure 3.

The chosen plants were indeed extreme phenotypes from the same population analysis done in a previous work (58), therefore were chosen after an extensive population phenotyping.

Plant phenotyping

Plant phenotyping was carried out using the same measurement methods from a previous work (38). The morphological parameters total height (cm), leaves (no.), nodes (no.), internodes (cm) and defoliation (1-no. leaves/no. nodes) were measured at days 0, 30, 45 and 60. Relative growth rate (RGR) was calculated as shown in the equation (1)

$$\text{Equation 1.} \qquad RGR = \frac{Ln(Height\ 2 - Height\ 1)}{t2 - t1}$$

Stem water potential (ψ_H, MPa) was measured in fully expanded leaves using a Model 600 Schölander Pressure Chamber (PMS Instrument Company, Albany, OR, USA). Measured leaves were kept in reflective plastic bags for 30 minutes (Levin, 2019). Measurements of leaf net CO_2 assimilation rate (A_{CO2}), leaf transpiration rate (E), internal CO_2 concentration (C_i) and stomatal conductance (g_s) were measured on three single leaves of each plant. Determinations were performed in fully expanded leaves from the mid-stem zone. The A_{CO2} and g_s ratio was used for Intrinsic leaf water use efficiency (WUE) calculation. The measurements were made using a CIRAS-2 Portable Photosynthesis System (PP Systems, Amesbury, Massachusetts, USA) using a PLC 6 (U) universal leaf autocuvette in a closed-circuit model and kept at 25 ± 0.5 ºC, with a leaf-to-air vapor deficit of about 1.7 kPa. The photosynthetically active radiation (PAR) was adjusted to 1.000 µmol m^{-2} s^{-1}photon flux density and the air flow rate through the cuvette was 0.5–1.5 L min^{-1}. The measurements were made in a sunny day between 9:30 a.m. and 12:30 p.m. at the end of the salt treatment (day 60).

After saline treatment, three leaves from each plant were collected. Sample pre-treatments were performed as described previously (38). Na^+, Ca^{2+}, K^+, Mg^{2+}, P and S content was determined using a multiple-collector inductively coupled plasma mass spectrometry (MC-ICP MS, Thermo Finnigan Neptune). Chloride concentration was quantified by silver ion-titration (68) with a Corning 926 automatic chloridometer (Corning Ltd. Halstead Essex, UK).

RNA extraction

After 60 days of salt treatment young fully expanded leaves and root tip tissue were collected and immediately frozen and powdered using liquid nitrogen. Control samples from all populations were also collected and processed. The samples of each of the three individuals were mixed. The three biological replicates were made resampling and mixing new tissue samples. RNA was isolated according to Gambino et al. (2008). DNA was removed with the RNase-Free DNase Set (Qiagen, Valencia, CA, USA), using the RNeasy Plant Mini Kit (Qiagen). Purified RNA (500 ng) was reverse transcribed with PrimeScript RT Reagent Kit (Takara Bio, Otsu, Japan) in a total volume of 10 µl.

RNA Sequencing

RNA samples were sequenced by Novogene® using the following procedure: mRNA was enriched using oligo(dT) beads and fragmented randomly using a fragmentation buffer. cDNA was synthetized using random hexamers and reverse transcriptase. A second strand was generated using nick-translation with RNAse H and Escherichia coli Polymerase I with Illumina second strand synthesis buffer and dNTPs. AMPure XP beads were used to purify the cDNA and the first strand was degraded with USER enzyme. Then, the resulting cDNA was purified, terminal repaired, A-tailed, ligated to the sequencing adapters, size-selected and enriched with PCR. The resulting library was sequence using Illumina.

Pre-processing of RNA-Seq data

The data pre-processing was performed as described here: http://www.epigenesys.eu/en/protocols/bio-informatics/1283-guidelines-for-rna-seq-data-analysis. Briefly, the quality of the raw sequence data was assessed using FastQC (http://www.bioinformatics.babraham.ac.uk/projects/fastqc/). Residual ribosomal RNA (rRNA) contamination was assessed and filtered using SortMeRNA (v2.1; settings –log –paired_in –fastx–sam –num_alignments 1) (70) using the rRNA sequences provided with SortMeRNA. Data was subsequently trimmed for adapters and quality using Trimmomatic (v0.36; settings TruSeq3-PE-2.fa:2:30:10 LEADING:3 SLIDINGWINDOW:5:20 MINLEN:50) (71). After both filtering steps, FastQC was run again to ensure that no technical artefacts were introduced.

Transcriptome de novo assembly and annotation

As there was no transcriptome assembly for any *Diospyros* species, a *de novo* transcriptome was built using the sequences from the RNA-Seq data. For transcriptome assembly, Trinity (v2.8.3.1) (72) was used inside a Singularity (v2.5.2) (73) container for ensuring reproducibility. Protein sequences were also putatively predicted. Assembled transcriptome was then annotated using Blast2GO (74), Blast+ (v2.6.0; using blastp) (75) against UniRef90 database (10^{th} October 2018) (76), HMMER (v3.1) (http://hmmer.org/), Trinotate (77), PFAM (v3.1;) (78) and signalP (Trinity package v.2.8.3.1) (72).

Differential expression analyses

Filtered reads were pseudo-aligned to the obtained transcriptome using kallisto (v0.44, non-default settings: -b 100 –rf-stranded -t 8) (79). Statistical analysis of single-gene differential expression between conditions was performed in R (v3.6.0; R Core Team 2019) using the Bioconductor (v3.9) (80) DESeq2 package (v1.24.1) (81). FDR adjusted p-values were used to assess significance; a common threshold of 1% was used throughout. For the data quality assessment (QA) and visualisation, the read counts were normalised using a variance stabilising transformation as implemented in DESeq2. The biological relevance of the data - e.g. biological replicates similarity - was assessed by Principal Component Analysis (PCA) and other visualisations (e.g. heatmaps), using custom R scripts, available from https://github.com/fragimuo/Dateplum-salinity-tolerance-RNAseq/. The RAW data has been deposited at the ENA (European Nucleotide Archive, https://ebi.ac.uk/ena) under the accession number PRJEB39098

List Of Abbreviations

ABA: Abscisic Acid

BLAST: Basic Local Alignment Search Tool

CBL1: Calcineurin B-like protein 1

cDNA: Complementary DNA

CIPK: CBL-interacting serine/threonine-protein kinase

DNA: Deoxyribonucleic Acid

DNase: Deoxyribonuclease

ENA: European Nucleotide Archive

FC: Fold Change

FDR: False Discovery Rate

H^+/ATPase: Adenosine Triphosphate Phosphohydrolase (H+-exporting).

HKT: High Affinity Potassium Transporter

IVIA: Instituto Valenciano de Investigaciones Agrarias

MAPK: Mitogen-activated protein kinase

MC-ICP MS: Multiple-Collector Inductively Coupled Plasma Mass Spectrometry

mRNA: Messenger RNA

PCA: Principal Component Analysis

PCR: Polymerase Chain Reaction

PSI: Photosystem I

PSII: Photosystem II

QA: Quality Asessment

RGR: Relative Growth Ratio

RNA: Ribonucleic Acid

RNase: Ribonuclease

RNA-Seq: Ribonucleic Acid Sequencing

RT: Retrotranscription

SOS: Saline Overly Sensitive

WUE: Water Use Efficiency

Declarations

Ethics approval and consent to participate

Not applicable

Consent for publication

All authors approved the Manuscript

Availability of data and materials

All the scripts used in data processing are deposited in the following repository: https://github.com/fragimuo/Dateplum-salinity-tolerance-RNAseq/. The RAW data has been deposited at the ENA (European Nucleotide Archive, https://ebi.ac.uk/ena) under the accession number PRJEB39098.

Competing interests

The authors declare that they have no competing interests.

Funding

Francisco Gil-Muñoz was funded by a PhD fellowship co-financed by the European Social Fund and the Generalitat Valenciana, grant ACIF/2016/115 and BEFPI/2018/056). The project was funded by the IVIA

grant 51914. RGG was funded by a grant from OECD, Cooperative Research Programme. The funders did not participate in the design, tasks and development of the study.

Author Contributions

MLB and MMN contributed to the experimental design. FGM, AQ and MMN made the experiment, phenotypical analysis and sample collection. FGM and ND performed the bioinformatics data process and analysis. FGM, ND and RGG analysed the data. FGM, MLB and RGG wrote the paper. All authors reviewed and approved the manuscript.

Acknowledgements

Not applicable

References

1. Flowers TJ, Colmer TD. Salinity tolerance in halophytes. Vol. 179, New Phytologist. 2008. p. 945–63.
2. Munns R, Tester M. Mechanisms of Salinity Tolerance. Annu Rev Plant Biol [Internet]. 2008;59(1):651–81. Available from: http://www.annualreviews.org/doi/10.1146/annurev.arplant.59.032607.092911
3. Bose J, Rodrigo-Moreno A, Shabala S. ROS homeostasis in halophytes in the context of salinity stress tolerance. Vol. 65, Journal of Experimental Botany. 2014. p. 1241–57.
4. Libutti A, Cammerino ARB, Monteleone M. Risk assessment of soil salinization due to tomato cultivation in mediterranean climate conditions. Water (Switzerland). 2018;10(11).
5. Ashrai M, McNelly T. Improvement of Salt Tolerance in Maize by Selection and Breeding. Plant Breed [Internet]. 1990 Apr 1 [cited 2020 Apr 10];104(2):101–7. Available from: http://doi.wiley.com/10.1111/j.1439-0523.1990.tb00410.x
6. Saranga Y, Cahaner A, Zamir D, Marani A, Rudich J. Breeding tomatoes for salt tolerance: inheritance of salt tolerance and related traits in interspecific populations. Theor Appl Genet [Internet]. 1992 Jul [cited 2020 Apr 3];84(3–4):390–6. Available from: http://www.ncbi.nlm.nih.gov/pubmed/24203199
7. Cuartero J, Bolarín MC, Asíns MJ, Moreno V. Increasing salt tolerance in the tomato. J Exp Bot [Internet]. 2006 [cited 2020 Apr 10];57(5):1045–58. Available from: http://www.ncbi.nlm.nih.gov/pubmed/16520333
8. Forner-Giner MA, Ancillo G. Breeding salinity tolerance in citrus using rootstocks. In: Salt Stress in Plants: Signalling, Omics and Adaptations. 2013. p. 355–76.
9. Shahid MA, Balal RM, Khan N, Simón-Grao S, Alfosea-Simón M, Cámara-Zapata JM, et al. Rootstocks influence the salt tolerance of Kinnow mandarin trees by altering the antioxidant defense system, osmolyte concentration, and toxic ion accumulation. Sci Hortic (Amsterdam). 2019;250:1–11.

10. Daszkowska-Golec A, Szarejko I. Open or close the gate - Stomata action under the control of phytohormones in drought stress conditions. Vol. 4, Frontiers in Plant Science. Frontiers Research Foundation; 2013. p. 138.
11. Lim CW, Baek W, Jung J, Kim JH, Lee SC. Function of ABA in stomatal defense against biotic and drought stresses [Internet]. Vol. 16, International Journal of Molecular Sciences. MDPI AG; 2015 [cited 2020 Apr 10]. p. 15251–70. Available from: http://www.ncbi.nlm.nih.gov/pubmed/26154766
12. Tester M, Davenport R. Na+tolerance and Na+transport in higher plants. Vol. 91, Annals of Botany. 2003. p. 503–27.
13. Gong D, Guo Y, Jagendorf AT, Zhu JK. Biochemical characterization of the Arabidopsis protein kinase SOS2 that functions in salt tolerance. Plant Physiol. 2002;130(1):256–64.
14. Hsu JL, Wang LY, Wang SY, Lin CH, Ho KC, Shi FK, et al. Functional phosphoproteomic profiling of phosphorylation sites in membrane fractions of salt-stressed Arabidopsis thaliana. Proteome Sci. 2009;7:42.
15. Martínez-Atienza J, Jiang X, Garciadeblas B, Mendoza I, Zhu JK, Pardo JM, et al. Conservation of the salt overly sensitive pathway in rice. Plant Physiol. 2007;143(2):1001–12.
16. Volkov V. Salinity tolerance in plants. Quantitative approach to ion transport starting from halophytes and stepping to genetic and protein engineering for manipulating ion fluxes. Vol. 6, Frontiers in Plant Science. Frontiers Research Foundation; 2015. p. 873.
17. Yang Z, Li JL, Liu LN, Xie Q, Sui N. Photosynthetic Regulation Under Salt Stress and Salt-Tolerance Mechanism of Sweet Sorghum. Vol. 10, Frontiers in Plant Science. Frontiers Media S.A.; 2020. p. 1722.
18. Chen S, Wu F, Li Y, Qian Y, Pan X, Li F, et al. NTMYB4 and NTCHS1 are critical factors in the regulation of flavonoid biosynthesis and are involved in salinity responsiveness. Front Plant Sci [Internet]. 2019 Feb 21 [cited 2020 Apr 10];10:178. Available from: https://www.frontiersin.org/article/10.3389/fpls.2019.00178/full
19. Nguyen HM, Sako K, Matsui A, Suzuki Y, Mostofa MG, Van Ha C, et al. Ethanol enhances high-salinity stress tolerance by detoxifying reactive oxygen species in arabidopsis thaliana and rice. Front Plant Sci [Internet]. 2017 Jul 3 [cited 2020 Apr 10];8:1001. Available from: http://www.ncbi.nlm.nih.gov/pubmed/28717360
20. Tao JJ, Chen HW, Ma B, Zhang WK, Chen SY, Zhang JS. The role of ethylene in plants under salinity stress. Front Plant Sci. 2015;6(NOVEMBER):1–12.
21. Suzuki N, Bassil E, Hamilton JS, Inupakutika MA, Zandalinas SI, Tripathy D, et al. ABA is required for plant acclimation to a combination of salt and heat stress. Wu K, editor. PLoS One [Internet]. 2016 Jan 29 [cited 2020 Apr 10];11(1):e0147625. Available from: https://dx.plos.org/10.1371/journal.pone.0147625
22. Yu Z, Wang X, Zhang L. Structural and functional dynamics of dehydrins: A plant protector protein under abiotic stress. Vol. 19, International Journal of Molecular Sciences. MDPI AG; 2018.

23. Hanin M, Brini F, Ebel C, Toda Y, Takeda S, Masmoudi K. Plant dehydrins and stress tolerance: Versatile proteins for complex mechanisms [Internet]. Vol. 6, Plant Signaling and Behavior. 2011 [cited 2020 Apr 10]. p. 1503–9. Available from: http://www.ncbi.nlm.nih.gov/pubmed/21897131
24. Kapilan R, Vaziri M, Zwiazek JJ. Regulation of aquaporins in plants under stress. Vol. 51, Biological Research. BioMed Central Ltd.; 2018.
25. Boudsocq M, Laurière C. Osmotic signaling in plants. Multiple pathways mediated by emerging kinase families. Vol. 138, Plant Physiology. 2005. p. 1185–94.
26. Isah T. Stress and defense responses in plant secondary metabolites production. Vol. 52, Biological research. NLM (Medline); 2019. p. 39.
27. Quan R, Lin H, Mendoza I, Zhang Y, Cao W, Yang Y, et al. SCABP8/CBL10, a putative calcium sensor, interacts with the protein kinase SOS2 to protect Arabidopsis shoots from salt stress. Plant Cell. 2007;19(4):1415–31.
28. Luo Y, Reid R, Freese D, Li C, Watkins J, Shi H, et al. Salt tolerance response revealed by RNA-Seq in a diploid halophytic wild relative of sweet potato. Sci Rep. 2017;7(1).
29. Shafi A, Zahoor I. Plant Survival and Tolerance Under High Salinity: Primary and Secondary Cell Wall-Sensing Mechanism. In: Salt Stress, Microbes, and Plant Interactions: Causes and Solution. 2019. p. 129–46.
30. Moustafa K, AbuQamar S, Jarrar M, Al-Rajab AJ, Trémouillaux-Guiller J. MAPK cascades and major abiotic stresses. Vol. 33, Plant Cell Reports. 2014. p. 1217–25.
31. Sinha AK, Jaggi M, Raghuram B, Tuteja N. Mitogen-activated protein kinase signaling in plants under abiotic stress. Vol. 6, Plant Signaling and Behavior. Taylor & Francis; 2011. p. 196–203.
32. Shi H, Ishitani M, Kim C, Zhu JK. The Arabidopsis thaliana salt tolerance gene SOS1 encodes a putative Na+/H+ antiporter. Proc Natl Acad Sci U S A [Internet]. 2000;97(12):6896–901. Available from: http://www.pnas.org/cgi/doi/10.1073/pnas.120170197
33. Liu J. The Arabidopsis thaliana SOS2 gene encodes a protein kinase that is required for salt tolerance. Proc Natl Acad Sci [Internet]. 2000;97(7):3730–4. Available from: http://www.pnas.org/cgi/doi/10.1073/pnas.060034197
34. Mahajan S, Pandey GK, Tuteja N. Calcium- and salt-stress signaling in plants: Shedding light on SOS pathway. Vol. 471, Archives of Biochemistry and Biophysics. 2008. p. 146–58.
35. Zhang H, Lv F, Han X, Xia X, Yin W. The calcium sensor PeCBL1, interacting with PeCIPK24/25 and PeCIPK26, regulates Na+/K+ homeostasis in Populus euphratica. Plant Cell Rep. 2013;32(5):611–21.
36. Chen X, Huang Q, Zhang F, Wang B, Wang J, Zheng J. ZmCIPK21, a Maize CBL-Interacting Kinase, Enhances Salt Stress Tolerance in Arabidopsis Thaliana. Int J Mol Sci. 2014;15(8):14819–34.
37. Li R, Zhang J, Wu G, Wang H, Chen Y, Wei J. HbCIPK2, a novel CBL-interacting protein kinase from halophyte Hordeum brevisubulatum, confers salt and osmotic stress tolerance. Plant, Cell Environ. 2012;

38. Gil-Muñoz F, Pérez-Pérez JG, Quiñones A, Primo-Capella A, Cebolla J, Ángeles Forner-Giner M, et al. A cross population between D. Kaki and D. Virginiana shows high variability for saline tolerance and improved salt stress tolerance. Ng C, editor. PLoS One [Internet]. 2020 Feb 25 [cited 2020 Mar 10];15(2):e0229023. Available from: https://dx.plos.org/10.1371/journal.pone.0229023
39. Garciadeblás B, Senn ME, Bañuelos MA, Rodríguez-Navarro A. Sodium transport and HKT transporters: The rice model. Plant J. 2003;34(6):788–801.
40. Huang S, Spielmeyer W, Lagudah ES, James RA, Platten JD, Dennis ES, et al. A sodium transporter (HKT7) is a candidate for Nax1, a gene for salt tolerance in durum wheat. Plant Physiol. 2006;142(4):1718–27.
41. Horie T, Costa A, Kim TH, Han MJ, Horie R, Leung HY, et al. Rice OsHKT2;1 transporter mediates large Na+ influx component into K+-starved roots for growth. EMBO J. 2007;26(12):3003–14.
42. Almeida P, Katschnig D, de Boer AH. HKT transporters-state of the art. Vol. 14, International Journal of Molecular Sciences. 2013. p. 20359–85.
43. Isayenkov S V., Maathuis FJM. Plant salinity stress: Many unanswered questions remain. Vol. 10, Frontiers in Plant Science. 2019.
44. Besada C, Gil R, Bonet L, Quiñones A, Intrigliolo D, Salvador A. Chloride stress triggers maturation and negatively affects the postharvest quality of persimmon fruit. Involvement of calyx ethylene production. Plant Physiol Biochem. 2016;100:105–12.
45. Formentin E, Sudiro C, Perin G, Riccadonna S, Barizza E, Baldoni E, et al. Transcriptome and cell physiological analyses in different rice cultivars provide new insights into adaptive and salinity stress responses. Front Plant Sci. 2018 Mar 5;9:204.
46. Tian X, Wang Z, Zhang Q, Ci H, Wang P, Yu L, et al. Genome-wide transcriptome analysis of the salt stress tolerance mechanism in Rosa chinensis. Amancio S, editor. PLoS One [Internet]. 2018 Jul 26 [cited 2020 Mar 31];13(7):e0200938. Available from: https://dx.plos.org/10.1371/journal.pone.0200938
47. Wang J, Zhu J, Zhang Y, Fan F, Li W, Wang F, et al. Comparative transcriptome analysis reveals molecular response to salinity stress of salt-tolerant and sensitive genotypes of indica rice at seedling stage. Sci Rep. 2018 Dec 1;8(1):1–13.
48. Zeng A, Chen P, Korth KL, Ping J, Thomas J, Wu C, et al. RNA sequencing analysis of salt tolerance in soybean (Glycine max). Genomics. 2019 Jul 1;111(4):629–35.
49. Amirbakhtiar N, Ismaili A, Ghaffari MR, Firouzabadi FN, Shobbar ZS. Transcriptome response of roots to salt stress in a salinity-tolerant bread wheat cultivar. Jain M, editor. PLoS One [Internet]. 2019 Mar 15 [cited 2020 Mar 31];14(3):e0213305. Available from: http://dx.plos.org/10.1371/journal.pone.0213305
50. Palmgren MG. Plant Plasma Membrane H+/-ATPases: Powerhouses for Nutrient Uptake. Annu Rev Plant Physiol Plant Mol Biol [Internet]. 2001 Jun [cited 2020 Apr 10];52(1):817–45. Available from: http://www.ncbi.nlm.nih.gov/pubmed/11337417

51. Niu X, Narasimhan ML, Salzman RA, Bressan RA, Hasegawa PM. NaCl regulation of plasma membrane H+-ATPase gene expression in a glycophyte and a halophyte. Plant Physiol. 1993;
52. Vera-Estrella R, Barkla BJ, Higgins VJ, Blumwald E. Plant defense response to fungal pathogens. Activation of host-plasma membrane H+-ATPase by elicitor-induced enzyme dephosphorylation. Plant Physiol. 1994;
53. Chen Z, Pottosin II, Cuin TA, Fuglsang AT, Tester M, Jha D, et al. Root plasma membrane transporters controlling K+/Na+ homeostasis in salt-stressed barley. Plant Physiol. 2007;145(4):1714–25.
54. Sahu BB, Shaw BP. Salt-inducible isoform of plasma membrane H+ATPase gene in rice remains constitutively expressed in natural halophyte, Suaeda maritima. J Plant Physiol. 2009;
55. Gévaudant F, Duby G, Von Stedingk E, Zhao R, Morsomme P, Boutry M. Expression of a constitutively activated plasma membrane H +-ATPase alters plant development and increases salt tolerance. Plant Physiol. 2007;
56. Shen P, Wang R, Jing W, Zhang W. Rice Phospholipase Dα is Involved in Salt Tolerance by the Mediation of H+-ATPase Activity and Transcription. J Integr Plant Biol. 2011;
57. de Paz JM, Visconti F, Chiaravalle M, Quiñones A. Determination of persimmon leaf chloride contents using near-infrared spectroscopy (NIRS). Anal Bioanal Chem. 2016;408(13):3537–45.
58. Gil-Muñoz F, Pérez-Pérez JG, Quiñones A, Naval M del M, Badenes ML. Intra and Inter-specific Variability of Salt Tolerance Mechanisms in Diospyros Genus. Front Plant Sci [Internet]. 2020 Aug 7 [cited 2020 Aug 10];11:1132. Available from: https://www.frontiersin.org/article/10.3389/fpls.2020.01132/full
59. Petrov V, Hille J, Mueller-Roeber B, Gechev TS. ROS-mediated abiotic stress-induced programmed cell death in plants [Internet]. Vol. 6, Frontiers in Plant Science. Frontiers Research Foundation; 2015 [cited 2020 Apr 10]. p. 69. Available from: http://www.ncbi.nlm.nih.gov/pubmed/25741354
60. Baetz U, Eisenach C, Tohge T, Martinoia E, De Angeli A. Vacuolar chloride fluxes impact ion content and distribution during early salinity stress. Plant Physiol [Internet]. 2016;172(2):1167–81. Available from: http://www.plantphysiol.org/lookup/doi/10.1104/pp.16.00183
61. Tong W, Yoshimoto K, Kakehi J-I, Motose H, Niitsu M, Takahashi T. Thermospermine modulates expression of auxin-related genes in Arabidopsis. Front Plant Sci [Internet]. 2014 Mar 14 [cited 2020 Apr 10];5(MAR):94. Available from: http://journal.frontiersin.org/article/10.3389/fpls.2014.00094/abstract
62. Osakabe Y, Arinaga N, Umezawa T, Katsura S, Nagamachi K, Tanaka H, et al. Osmotic stress responses and plant growth controlled by potassium transporters in Arabidopsis. Plant Cell. 2013 Feb;25(2):609–24.
63. Julkowska MM, Hoefsloot HCJ, Mol S, Feron R, De Boer GJ, Haring MA, et al. Capturing arabidopsis root architecture dynamics with root-fit reveals diversity in responses to salinity. Plant Physiol. 2014 Nov 1;166(3):1387–402.
64. Julkowska MM, Koevoets IT, Mol S, Hoefsloot H, Feron R, Tester MA, et al. Genetic components of root architecture remodeling in response to salt stress. Plant Cell. 2017 Dec 1;29(12):3198–213.

65. Incesu M, Cimen B, Yesiloglu T, Yilmaz B. Growth and photosynthetic response of two persimmon rootstocks (Diospyros kaki and D. virginiana) under different salinity levels. Not Bot Horti Agrobot Cluj-Napoca. 2014;42(2):386–91.
66. Intrigliolo DS, Visconti F, Bonet L, Parra M, Besada C, Abrisqueta I, et al. Persimmon (Diospyros kaki) trees responses to restrictions in water amount and quality. In: Water Scarcity and Sustainable Agriculture in Semiarid Environment: Tools, Strategies, and Challenges for Woody Crops. Elsevier; 2018. p. 149–77.
67. Visconti F, Intrigliolo DS, Quiñones A, Tudela L, Bonet L, de Paz JM. Differences in specific chloride toxicity to Diospyros kaki cv. “Rojo Brillante” grafted on D. lotus and D. virginiana. Sci Hortic (Amsterdam). 2017;214:83–90.
68. Gilliam JW. Rapid Measurement of Chlorine in Plant Materials1. Soil Sci Soc Am J [Internet]. 1971;35(3):512. Available from: https://www.soils.org/publications/sssaj/abstracts/35/3/SS0350030512
69. Gambino G, Perrone I, Gribaudo I. A rapid and effective method for RNA extraction from different tissues of grapevine and other woody plants. Phytochem Anal. 2008;19(6):520–5.
70. Kopylova E, Noé L, Touzet H. SortMeRNA: Fast and accurate filtering of ribosomal RNAs in metatranscriptomic data. Bioinformatics. 2012;
71. Bolger AM, Lohse M, Usadel B. Trimmomatic: A flexible trimmer for Illumina sequence data. Bioinformatics. 2014;
72. Haas BJ, Papanicolaou A, Yassour M, Grabherr M, Blood PD, Bowden J, et al. De novo transcript sequence reconstruction from RNA-seq using the Trinity platform for reference generation and analysis. Nat Protoc. 2013;
73. Kurtzer GM, Sochat V, Bauer MW. Singularity: Scientific containers for mobility of compute. PLoS One. 2017;
74. Conesa A, Götz S, García-Gómez JM, Terol J, Talón M, Robles M. Blast2GO: A universal tool for annotation, visualization and analysis in functional genomics research. Bioinformatics. 2005;
75. Camacho C, Coulouris G, Avagyan V, Ma N, Papadopoulos J, Bealer K, et al. BLAST+: Architecture and applications. BMC Bioinformatics. 2009;
76. Suzek BE, Wang Y, Huang H, McGarvey PB, Wu CH. UniRef clusters: A comprehensive and scalable alternative for improving sequence similarity searches. Bioinformatics. 2015;
77. Bryant DM, Johnson K, DiTommaso T, Tickle T, Couger MB, Payzin-Dogru D, et al. A Tissue-Mapped Axolotl De Novo Transcriptome Enables Identification of Limb Regeneration Factors. Cell Rep. 2017;
78. El-Gebali S, Mistry J, Bateman A, Eddy SR, Luciani A, Potter SC, et al. The Pfam protein families database in 2019. Nucleic Acids Res. 2019;
79. Bray NL, Pimentel H, Melsted P, Pachter L. Near-optimal probabilistic RNA-seq quantification. Nat Biotechnol. 2016;

80. Gentleman RC, Carey VJ, Bates DM, Bolstad B, Dettling M, Dudoit S, et al. Bioconductor: open software development for computational biology and bioinformatics. Genome Biol. 2004;
81. Love MI, Anders S, Huber W. Differential analysis of count data - the DESeq2 package. Genome Biology. 2014.

Tables

Due to technical limitations, table 2,3,4 is only available as a download in the Supplemental Files section.

Figures

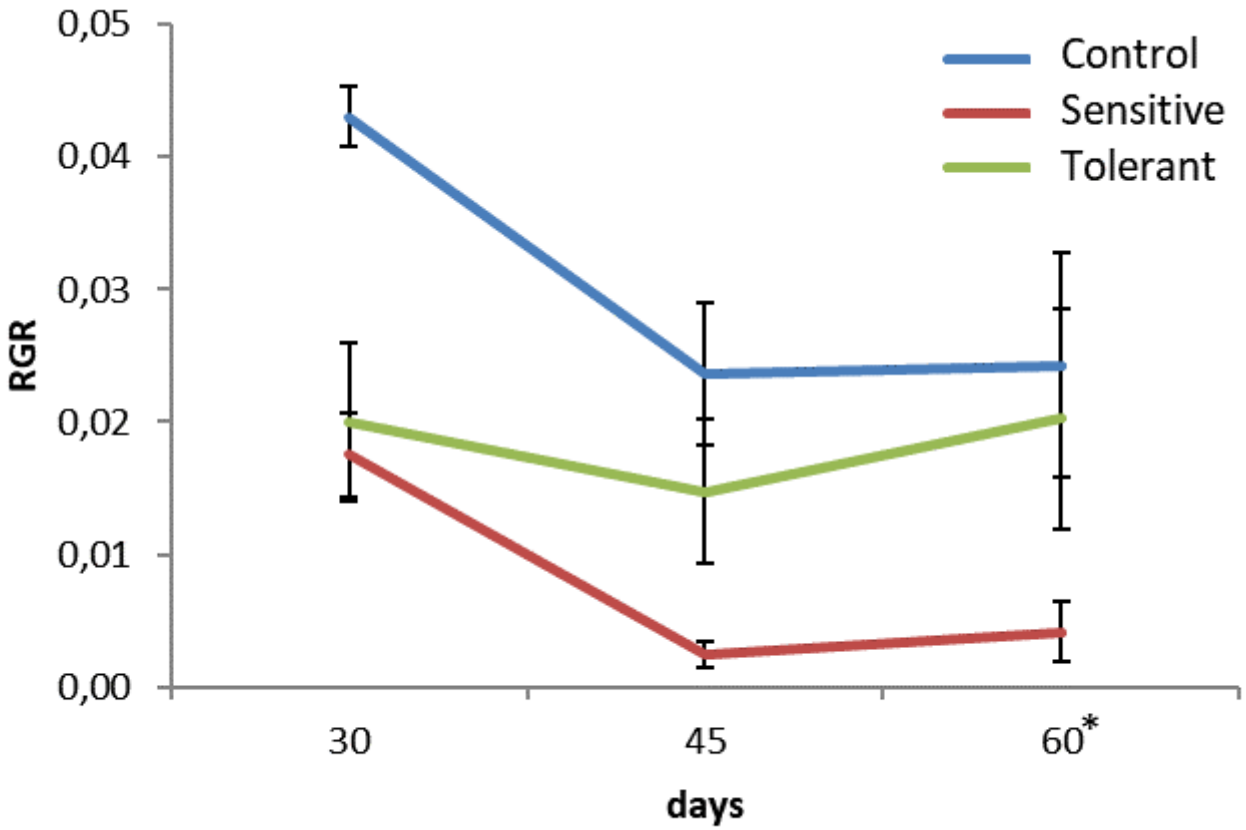

Figure 1

Relative growth rate (RGR) of the groups. Bar represents standard deviation. Asterisk (*) indicates significant differences between tolerant and sensitive groups (Kruskal-Wallis test, $p<0.05$).

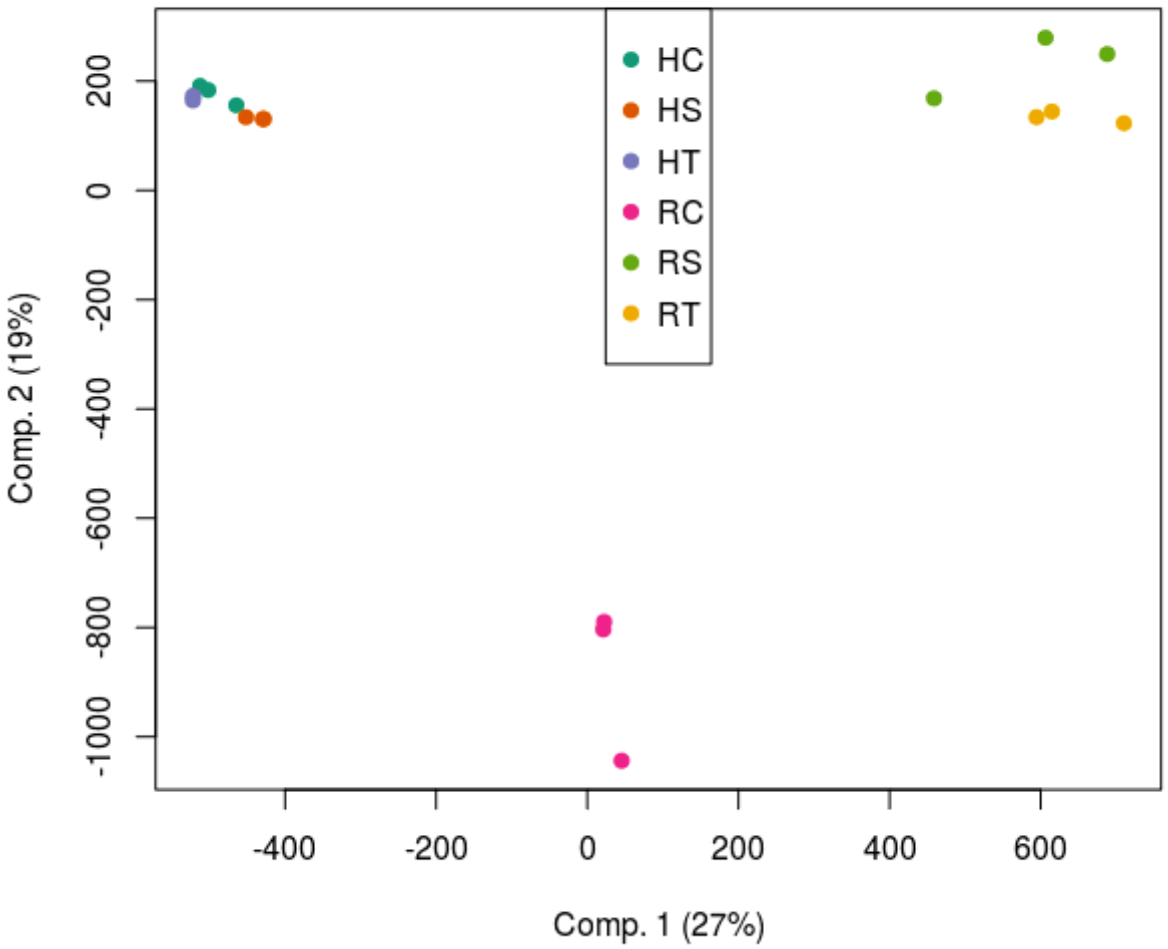

Figure 2

Principal component analysis of the whole transcriptomic profiles of the six analyzed samples with its three biological replicates

Supplementary Files

This is a list of supplementary files associated with this preprint. Click to download.

- SupplementaryfiguresS1S2andS3.docx
- Table2a.JPG
- Table2b.JPG
- Table2c.JPG
- Table3.JPG
- Table4.JPG